# A fluorescence study of ligand-induced conformational changes in cytosolic fructose-1,6-bisphosphatase from germinating castor oil seeds

**ARTICLE** *in* BIOCHIMICA ET BIOPHYSICA ACTA · DECEMBER 1998

Impact Factor: 4.66 · DOI: 10.1016/S0167-4838(98)00176-9 · Source: PubMed



**3 AUTHORS**, INCLUDING:

Richard J Hodgson
University Health Network
**19** PUBLICATIONS **433** CITATIONS
SEE PROFILE

William C Plaxton
Queen's University
**162** PUBLICATIONS **5,989** CITATIONS
SEE PROFILE

ELSEVIER

Biochimica et Biophysica Acta 1388 (1998) 285–294

BIOCHIMICA ET BIOPHYSICA ACTA
BBA

# A fluorescence study of ligand-induced conformational changes in cytosolic fructose-1,6-bisphosphatase from germinating castor oil seeds

Richard J. Hodgson [a], Zongchao Jia [b], William C. Plaxton [a, b,*]

[a] *Department of Biology, Queen's University, Kingston, Ontario K7L 3N6, Canada*
[b] *Department of Biochemistry, Queen's University, Kingston, Ontario K7L 3N6, Canada*

Received 18 March 1998; accepted 5 May 1998

**Abstract**

The intrinsic fluorescence of homogeneous castor oil seed cytosolic fructose-1,6-bisphosphatase ($FBPase_c$) was used as an indicator of conformational changes due to ligand binding. Binding of the substrate and the inhibitor fructose-2,6-bisphosphate (F-2,6-$P_2$) was quantitatively compared to their respective kinetic effects on enzymatic activity. There are two distinct types of substrate interaction with $FBPase_c$, corresponding to catalytic and inhibitory binding, respectively. Inhibitory substrate binding shares several characteristics with F-2,6-$P_2$ binding which indicates that both ligands bind at the same site. However, F-2,6-$P_2$ does not prevent fluorescence transitions attributed to catalytic substrate binding. The marked synergistic inhibition of $FBPase_c$ by AMP and F-2,6-$P_2$ appears to arise via AMP's promotion of F-2,6-$P_2$ binding. Based on the X-ray crystal structure of porcine kidney FBPase our modelling studies suggest the existence of a distinct F-1,6-$P_2$/F-2,6-$P_2$ inhibitory binding site which partially overlaps with the enzyme's catalytic site. We propose that a pronounced allosteric transition mediated by AMP binding increases access of F-1,6-$P_2$ and F-2,6-$P_2$ to this common inhibitory binding site. 

*Keywords:* Oil seed; Synergistic interaction; Enzyme regulation; Fructose-2,6-bisphosphate; Gluconeogenesis; Intrinsic fluorescence

## 1. Introduction

Fructose-1,6-bisphosphatase (FBPase; D-fructose-1,6-bisphosphate 1-phosphohydrolase, EC 3.1.3.11) is a key regulatory enzyme of the gluconeogenic pathway. In the presence of divalent metal cations such as $Mg^{2+}$ or $Mn^{2+}$, the enzyme catalyses the highly specific and essentially irreversible hydrolysis of F-1,6-$P_2$ to fructose-6-P and $P_i$. In all eukaryotes, FBPase is found in the cytosol, but in plants FBPase is also located in plastids. The enzyme has been purified and extensively characterized from a wide variety of non-plant sources where it usually exists as a homotetramer, with a subunit $M_r$ of 36–41 kDa [1]. Although FBPase activity follows typical hyperbolic substrate saturation kinetics at low F-1,6-$P_2$ concentrations, the Michaelis-Menten $V_{max}$ is not attained owing to the progressive inhibition that arises with increasing substrate concentrations [2,3]. Accurate determination of the enzyme's $K_m$ value for F-1,6-$P_2$ is problematic because it is very low, and reaction velocities measured at low F-1,6-$P_2$ concentrations

Abbreviations: COS, castor oil seed; F-1,6-$P_2$, fructose-1,6-bisphosphate; F-2,6-$P_2$, fructose-2,6-bisphosphate; FBPase, fructose-1,6-bisphosphatase (EC 3.1.3.11); $FBPase_c$ and $FBPase_p$, cytosolic and plastidic FBPase isozymes, respectively; NEM, *N*-ethylmaleimide; R-to-T, relaxed-to-tense

* Corresponding author, at address a. Fax: +1 (613) 5456617; E-mail: plaxton@biology.queensu.ca

0167-4838/98/$ – see front matter 
PII: S0167-4838(98)00176-9

may reflect a small component of substrate inhibition [2–4].

An important regulatory characteristic shared by animal and yeast FBPases is their potent synergistic inhibition by F-2,6-$P_2$ and AMP [1]. Because F-2,6-$P_2$ is a potent activator of many phosphofructokinases, it is believed that this regulatory metabolite plays a critical role in the coordinate regulation of glycolysis and gluconeogenesis [5]. Although F-2,6-$P_2$ and AMP synergistically inhibit FBPase, the molecular basis for their synergism is unclear. NMR studies of AMP binding to mammalian FBPase indicated that F-2,6-$P_2$ enhances AMP binding [6]. By contrast, F-2,6-$P_2$ did not alter binding of a fluorescent AMP analogue, formycin A-5′-P, to the mammalian enzyme [7]. X-Ray crystallographic studies of porcine kidney FBPase have revealed that: (i) a relaxed-to-tense (R-to-T) state transition is triggered by binding of AMP to a distal allosteric site that is approx. 30 Å from the substrate binding site [8], and (ii) F-2,6-$P_2$ binds at the active site and does not elicit the R-to-T transitions observed with AMP [9,10]. Although the X-ray crystal structure data are compelling, mammalian FBPase displays several properties which it cannot account for. For example, chemical modification of FBPase with the sulfhydryl reagent NEM yields an active enzyme which was insensitive to F-2,6-$P_2$, suggesting that F-2,6-$P_2$ binds at an allosteric site [11–13]. Moreover, as the NEM-modified enzyme was not substrate inhibited, substrate inhibition may arise from F-1,6-$P_2$ binding at the F-2,6-$P_2$ allosteric site.

Plastidic and cytosolic FBPase isozymes ($FBPase_p$ and $FBPase_c$, respectively) have been identified in plant tissues [14]. $FBPase_p$ of photosynthetic tissues plays an important function in the regulation of the reductive pentose-*P* pathway (Calvin cycle), is reversibly light-activated by the ferredoxin-thioredoxin system, but is not regulated by F-2,6-$P_2$ or AMP [14]. Plant $FBPase_c$ is a key enzyme in the sucrose biosynthetic pathway, catalysing the first irreversible reaction in the conversion of triose-*P* to sucrose. As is the case with animal and yeast FBPase, plant $FBPase_c$ exhibits potent synergistic inhibition by F-2,6-$P_2$ and AMP, and substrate inhibition by F-1,6-$P_2$ [14]. Plant $FBPase_c$ is immunologically related to mammalian FBPase, but not to $FBPase_p$ [15]. This agrees with the observation that the derived primary structure of plant $FBPase_c$ shows closer homology to that of other eukaryotic non-plant FBPases, than it does to $FBPase_p$ [14].

Germinating castor oil seed (COS) endosperm represents an excellent model system for the study of $FBPase_c$ from a non-photosynthetic plant tissue. The aerobic metabolism of germinating COS is dominated by the transformation of reserve lipids into sucrose, a process that involves the gluconeogenic conversion of phospho*enol*pyruvate derived from fatty acids into hexose mono-P [16,17]. The extractable activity of COS $FBPase_c$ is similar to that of mammalian muscle [1,4], and it is possible to isolate milligram amounts of homogeneous COS $FBPase_c$ [4,15].

The use of plant $FBPase_c$ for the study of its complex regulation allows the application of biophysical methods unavailable to those studying mammalian FBPase. Although the primary structure of COS $FBPase_c$ has not been determined, the observed fluorescence intensity of the purified enzyme indicates the presence of tryptophan [4,15]. This is consistent with the derived primary structure of $FBPase_c$ from leaves of spinach [18], sugar beet [19], and potato [20] which uniformly demonstrate the existence of a single tryptophan residue (corresponding to phenylalanine-219 of pig kidney FBPase [21]). Intrinsic tryptophan fluorescence represents a valuable probe of protein structural dynamics since the fluorescence behaviour of a tryptophan residue mirrors its microenvironment in the native protein. The emission maximum of tryptophan varies from 320 to 350 nm when the residue is in a very strong hydrophobic environment versus an aqueous solution [22]. The fluorescence intensity decreases when the tryptophan residue has close contact with charged or polar groups [22]. Alterations in an enzyme's intrinsic fluorescence can be used to estimate ligand binding constants, in addition to the use of kinetic techniques [22,23]. By not relying on enzyme catalysis as an indicator, fluorescence techniques provide a more direct method of investigating quantitative ligand binding. Intrinsic fluorescence studies of non-plant FBPases have not been reported, likely because of the absence of tryptophan in the non-plant enzyme [1,21]. Although relatively low [4,15], the fluorescence intensity of the COS $FBPase_c$ is sufficient to examine conformational effects brought about by substrate and effector binding

and allows us to address some of the current discrepancies concerning structure-function aspects of this enzyme. Kinetic and fluorescence data are compared for the purpose of clarifying the mechanism of $FBPase_c$ inhibition by F-1,6-$P_2$, F-2,6-$P_2$ and AMP. Re-examination of the X-ray crystal structure of pig kidney FBPase suggests a model for the interaction of the substrate and F-2,6-$P_2$ with eukaryotic FBPases which is consistent with all of the available data.

## 2. Materials and methods

### 2.1. Chemicals and plant material

Biochemicals and coupling enzymes were purchased from Sigma (St. Louis, MO, USA) while bis-Tris-propane was from Research Organics (Cleveland, OH, USA). All other reagents were of analytical grade and were purchased from BDH (Toronto, ON, Canada). F-1,6-$P_2$ was acid treated [15] to remove contaminating traces of F-2,6-$P_2$ and its concentration was verified spectrophotometrically [24].

Seeds of the castor plant (*Ricinus communis* L., cv. Hale), purchased from Bothwell Enterprises (Plainview, TX, USA) were germinated for 5 days as described in [15], dissected free from hypocotyls and the endosperms stored at −80°C until needed. The neutral (non-proteolytic degraded) form of COS $FBPase_c$ was purified to homogeneity as previously reported [15] with the modifications described in [4]. Typical values for the specific activity for the purified enzyme were around 70 μmol/min per mg protein at pH 7.5 and 30°C.

### 2.2. Enzyme assay and kinetic studies

$FBPase_c$ activity was monitored at 30°C by following the reduction of $NAD^+$ at 340 nm using a Gilford recording spectrophotometer. Standard assay conditions were: 50 mM bis-Tris-propane/HCl (pH 7.5), 50 μM F-1,6-$P_2$, 5 mM $MgCl_2$, 0.2 mM EGTA, 0.15 mM $NAD^+$, 1 mM DTT, 5% (w/v) polyethylene glycol (average $M_r$ 8000) and 1 unit each of desalted yeast hexose-*P* isomerase and *Leuconostoc mesenteroides* glucose-6-*P* dehydrogenase. Our previous study [4] demonstrated that 5% (w/v) polyethylene glycol significantly enhances the activity of homogeneous COS $FBPase_c$ by stabilizing the active tetrameric native structure and intrinsic fluorescence of the enzyme in dilute solutions. This organic cosolute was therefore routinely added to the buffers used for FBPase kinetic and intrinsic fluorescence studies. Assays were initiated by the addition of 0.1 μg of purified $FBPase_c$ and were linear with respect to time and enzyme concentration. One unit of FBPase activity is defined as the amount of enzyme resulting in the production of 1 μmol of fructose-6-P/min.

$I_{50}$ values (inhibitor concentration producing half-maximal inhibition of enzyme activity) and Hill coefficients were calculated using a non-linear least-squares computer kinetics program [25]. Stock solutions of metabolites were adjusted to pH 7.5. The concentration of AMP was verified spectrophotometrically using a published extinction coefficient [26].

### 2.3. Fluorescence measurements

The intrinsic fluorescence of COS $FBPase_c$ was determined on a Perkin-Elmer LS-50 spectrofluorometer using a 0.15 ml quartz micro-cuvette thermostatted at 30°C. Prior to each measurement the COS $FBPase_c$ was diluted to 57 μg/ml in 50 mM bis-Tris-propane/HCl (pH 7.5) containing 1 mM DTT and 5% (w/v) polyethylene glycol (average $M_r$ 8000) in a final volume of 125 μl. Emission spectra were corrected using buffer as blank. $FBPase_c$ steady-state intrinsic fluorescence was routinely determined by exciting at 280 nm (slit width 10 nm) and detecting the fluorescence emission at 334 nm (slit width 10 nm). Additions of ligands from concentrated stock solutions were made in 1 μl increments using a 10 μl Hamilton syringe. The maximum volume increase due to the sequential addition of the ligand stock solution was less than 5%. All results were corrected for dilution due to ligand addition. At the concentrations of protein or other additions used, no corrections were necessary due to inner filter effect. The change in fluorescence intensity at 334 nm was measured as a function of ligand concentration. However, fluorescence emission spectra from 300 to 400 nm were also analysed before and after ligand titrations to determine whether any shifts in emission maxima had occurred. All solutions were filtered

through 0.22 μm membranes prior to use. The Perkin-Elmer FL Data Manager (version 3.0) was used to acquire the data. The data were analysed by non-linear least-squares fitting according to the equation:

$$\Delta F/F_0 = \frac{(\Delta F_{max}/F_0) \times S^h}{K_d + S^h} \quad (1)$$

where $\Delta F$ is the change in fluorescence caused by a determined amount of ligand $S$, $F_0$ is the fluorescence in the absence of $S$, $K_d$ is the dissociation constant, and $h$ is the Hill coefficient.

## 3. Results

The COS $FBPase_c$ exhibited a broad pH activity profile with maximum activity occurring from pH 7.5 to 8.3 (data not shown). All subsequent kinetic and fluorometric studies were carried out at the physiologically relevant pH 7.5.

Consistent with our earlier studies [4,15], the COS $FBPase_c$ exhibited a broad fluorescence emission spectrum centred at 334 nm when excited at 280 nm. Fig. 1 presents the effect of F-1,6-$P_2$ and F-2,6-$P_2$ on $FBPase_c$'s fluorescence emission spectrum. Both ligands caused alterations in the enzyme's intrinsic fluorescence, but the spectral changes were not identical for each. F-1,6-$P_2$ caused two types of fluorescence changes depending on its concentration. F-1,6-$P_2$ at 50 μM produced a small, but statistically significant ($P < 0.005$, Student's $t$-test, $n = 3$), increase in fluorescence, whereas 1 mM F-1,6-$P_2$ caused fluorescence quenching, analogous to the effect of 2 μM F-2,6-$P_2$ (Fig. 1). In contrast to the other ligands, AMP produced a severe inner filter effect as it absorbs 280 nm (but not 295 nm) light at concentrations required for significant $FBPase_c$ inhibition. Although measurable fluorescence emission of the COS $FBPase_c$ could also be detected at 334 nm following excitation at 295 nm (results not shown), the signal to noise ratio was too low under these conditions to permit the use of intrinsic tryptophan fluorescence as an accurate probe for AMP-induced conformational changes. Unlike AMP, F-1,6-$P_2$ and F-2,6-$P_2$ exerted no influence on the fluorescence of free tryptophan following excitation at 280 nm (results not shown).

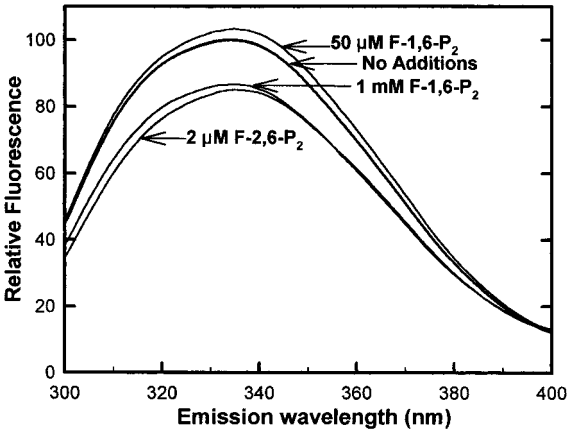


Fig. 1. The effect of various ligands on the fluorescence emission spectra of 8.5 μg (0.06 nmol) of homogeneous COS $FBPase_c$. Spectra are averages of triplicate determinations and were corrected for blank fluorescence and dilution due to ligand addition. All emission spectra were recorded using an excitation wavelength of 280 nm (slit width 10 nm) and detecting emission between 300 and 400 nm (slit width 10 nm) as described in Section 2.

Substrate saturation curves for the COS $FBPase_c$ in the absence and presence of F-2,6-$P_2$ or AMP are shown in Fig. 2A. The enzyme's $K_m$(F-1,6-$P_2$) in the absence of effectors was previously estimated to be 0.6 μM [4]. In accordance with previous studies [2–4], the enzyme was inhibited by high F-1,6-$P_2$ concentrations. The inhibitors each produced a unique effect on COS $FBPase_c$ substrate saturation kinetics (Fig. 2A). AMP (150 μM) caused a slight but statistically significant reduction in apparent $V_{max}$ ($P < 0.01$, Student's $t$-test, $n = 3$), which appears to be related to increased substrate inhibition, as reflected by the enzyme's reduced activity in the range of 50–150 μM F-1,6-$P_2$. In contrast, 0.5 μM F-2,6-$P_2$ markedly reduced both apparent $V_{max}$ and affinity for F-1,6-$P_2$. Notably, little substrate inhibition was observed in the presence of 0.5 μM F-2,6-$P_2$, and the apparent $V_{max}$ obtained in its presence was similar to the activity observed at high F-1,6-$P_2$ concentrations in the absence of added effectors (Fig. 2A). No substrate inhibition was observed in the presence of 25 μM F-2,6-$P_2$ (results not shown).

Progressive titration of the enzyme with F-1,6-$P_2$ yielded a small, but statistically significant ($P < 0.005$, Student's $t$-test, $n = 6$), increase in fluorescence intensity at low concentrations, followed by a larger decrease at higher concentrations (Fig. 2B). It is notable that this increase and decrease in $FBPase_c$

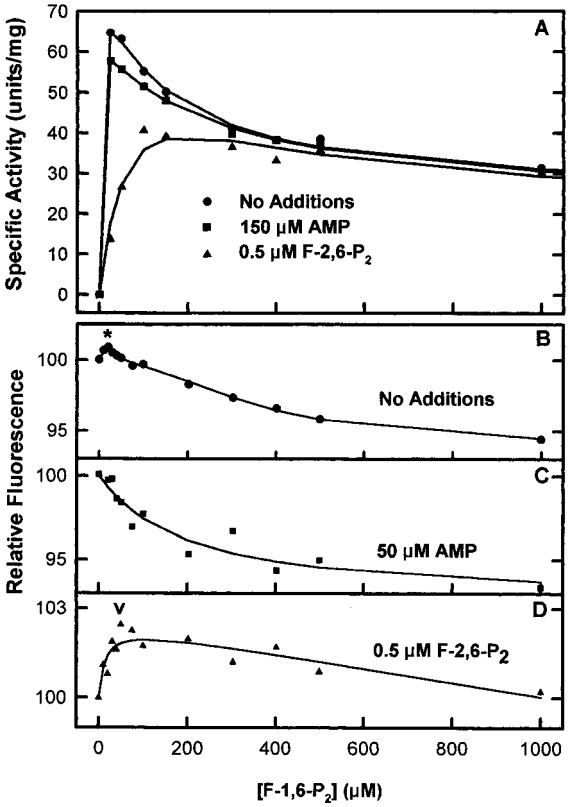


Fig. 2. Dependence of $FBPase_c$ activity (A) and intrinsic fluorescence (B,C,D) on the concentration of F-1,6-$P_2$, in the presence and absence of ligands as shown. Intrinsic fluorescence in the absence of F-1,6-$P_2$ was normalized to 100% for each respective plot. The intrinsic fluorescence measured at 20 μM F-1,6-$P_2$ in the absence of other ligands (B, marked with *) was significantly greater than that measured in the absence of F-1,6-$P_2$ ($P<0.005$, Students $t$-test, $n=6$). The intrinsic fluorescence measured at 50 μM F-1,6-$P_2$ in the presence of 0.5 μM F-2,6-$P_2$ (D, marked with v) was significantly greater than that measured in the absence of F-1,6-$P_2$ ($P<0.005$, Students $t$-test, $n=6$). $FBPase_c$ intrinsic fluorescence measured at high F-1,6-$P_2$ concentrations in the absence and presence of 50 μM AMP (B and C, respectively) was significantly less than the corresponding fluorescence measured in the absence of F-1,6-$P_2$ ($P<0.001$, Students $t$-test, $n=3$). Fluorescence measurements were corrected for dilution, and blank titrations did not lead to a measurable change in fluorescence. All results are the means of at least three independent determinations.

fluorescence intensity occurred at F-1,6-$P_2$ concentrations corresponding to increasing enzyme activity (catalytic substrate binding) and substrate inhibition (inhibitory substrate binding), respectively (Fig. 2A,B). The presence of 50 μM AMP only resulted in fluorescence quenching due to increasing concentrations of F-1,6-$P_2$ (Fig. 2C). By contrast, a small but statistically significant ($P<0.005$, Student's $t$-test, $n=6$) increase in fluorescence due to F-1,6-$P_2$ binding was observed in the presence of 0.5 μM F-2,6-$P_2$ (Fig. 2D). This increase in fluorescence occurred at F-1,6-$P_2$ concentrations corresponding to increasing activity (catalytic substrate binding) during assays with 0.5 μM F-2,6-$P_2$ (Fig. 2A,D).

Increasing concentrations of AMP potently inhibited enzymatic activity (Fig. 3). In the absence of F-2,6-$P_2$ the inhibition plot with AMP was sigmoidal in shape and yielded a Hill coefficient $>2$ (Fig. 3, Table 1). Synergistic inhibition by AMP and F-2,6-$P_2$, characteristic of $FBPase_c$, can be seen in Figs. 3 and 4A. F-2,6-$P_2$ at 0.5 μM decreased the enzyme's $I_{50}$(AMP) value by over 10-fold (Table 1). Marked absorbance of 280 nm light by AMP prevented the use of intrinsic fluorescence to assess AMP binding to the COS $FBPase_c$. Formycin A-5′-P, a fluorescent AMP analogue previously employed to estimate AMP binding to mammalian $FBPase_c$ [7], did not inhibit COS $FBPase_c$ and was therefore unsuitable. Another fluorescent AMP analogue, 1,$N^6$-etheno-AMP, was found to synergistically inhibit $FBPase_c$ ($I_{50}=1.5$ and 0.52 mM in the absence and presence of 0.5 μM F-2,6-$P_2$, respectively), but no change in its fluorescence emission spectrum was observed upon the addition of 4 μM $FBPase_c$. Similarly, we were unable to measure AMP binding to the COS $FBPase_c$ following chemical modification of the en-

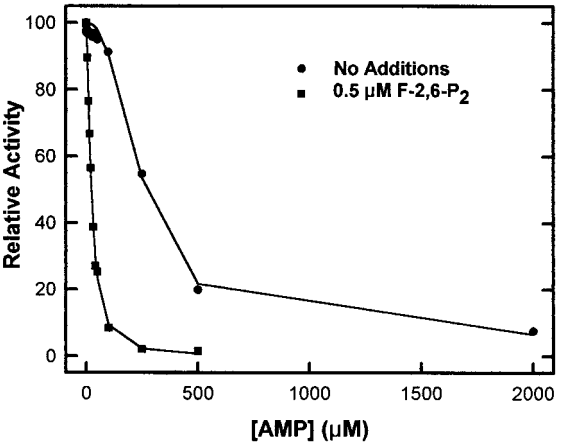


Fig. 3. Dependence of $FBPase_c$ activity on the concentration of AMP, in the presence and absence of 0.5 μM F-2,6-$P_2$. Activity was determined at 50 μM F-1,6-$P_2$. Activity in the absence of AMP was normalized to 100% for each plot. All results are the mean of three independent determinations.

zyme with the extrinsic fluorophors, fluorescein isothiocyanate or 8-anilino-1-naphthelenesulphonate.

The enzyme was markedly inhibited by low concentrations of F-2,6-$P_2$ (Fig. 4A). The inhibitory effect of F-2,6-$P_2$ was significantly enhanced by the addition of 50 μM AMP which reduced the enzyme's $I_{50}$(F-2,6-$P_2$) value by almost 2-fold (Fig. 4A, Table 1). Increasing concentrations of F-2,6-$P_2$ resulted in $>10\%$ fluorescence quenching (Fig. 4B). However, 50 μM AMP considerably enhanced the binding of F-2,6-$P_2$ (Fig. 4B) as reflected by the approx. 2-fold reduction in the $K_d$(F-2,6-$P_2$) value in its presence (Table 1). The addition of 1 mM F-1,6-$P_2$ negated $FBPase_c$ conformational changes due to F-2,6-$P_2$ (Fig. 4B). Likewise, 0.5 μM F-2,6-$P_2$ caused no change in $FBPase_c$ activity at 1 mM F-1,6-$P_2$ (Fig. 2A).

## 4. Discussion

### 4.1. Metabolic consequences of COS $FBPase_c$ kinetic properties

The kinetic properties of homogeneous COS $FBPase_c$ reported here are in general agreement with those previously determined for an impure preparation of the COS enzyme [27], and are strongly reminiscent of those obtained with FBPases from various non-plant eukaryotic sources [1–3,28]. One of the most striking kinetic properties of COS $FBPase_c$, first observed with liver $FBPase_c$ [28], is the strong synergism between AMP and F-2,6-$P_2$. Low concentrations of either inhibitor potentiate the sensitivity of the COS $FBPase_c$ to the other (Figs. 3 and 4A). The $I_{50}$ values for AMP and F-2,6-$P_2$ (Table 1) are well within their estimated physiological concentrations in the plant cytosol [5,16].

It appears that AMP and F-2,6-$P_2$ are key metabolites in the reciprocal regulation of glycolysis and gluconeogenesis in germinating COS. Classical radiotracer studies by Canvin and Beevers [17] revealed that the maximal rate of gluconeogenic flux in germinating aerobic COS is about 10-fold that of glycolysis. However, gluconeogenesis is quickly suppressed when this tissue undergoes anaerobiosis, whereas glycolytic flux is enhanced [16,17]. These anoxia-induced metabolic changes are parallelled by significant increases in the levels of F-2,6-$P_2$ and

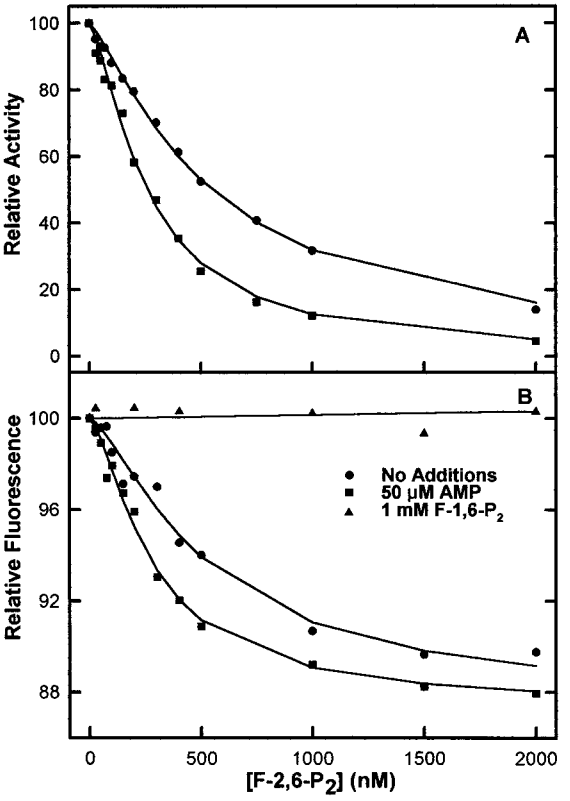


Fig. 4. Dependence of $FBPase_c$ activity (A) and intrinsic fluorescence (B) on the concentration of F-2,6-$P_2$, in the presence and absence of ligands as shown. Activity was determined at 50 μM F-1,6-$P_2$. Intrinsic fluorescence and activity in the absence of F-2,6-$P_2$ was normalized to 100% for each plot. All results are the mean of three independent determinations.

Table 1
Influence of various additions on binding constant ($K_d$) and/or $I_{50}$ values of COS $FBPase_c$ for AMP and F-2,6-$P_2$

| Effector | | Addition | | |
|---|---|---|---|---|
| | | None | 50 μM AMP | 0.5 μM F-2,6-$P_2$ |
| AMP | $I_{50}$ (μM) | 252 (2.34) | NA[a] | 22.8 (1.52) |
| F-2,6-$P_2$ | $K_d$ (nM) | 517 | 280 | NA |
| | $I_{50}$ (nM) | 551 | 259 | NA |

$K_d$ values were determined by fluorescence spectroscopy. $I_{50}$ values were determined using standard assay conditions (50 μM F-1,6-$P_2$) as described in Section 2. Hill coefficients were equivalent to 1.0 except where the value is indicated in parentheses. Each value is the mean of triplicate determinations with standard errors $<10\%$ of the mean.
[a]NA, not applicable.

AMP [16,29]. The parallel increases in the two $FBPase_c$ inhibitors provide a logical rationale for the inhibition of gluconeogenesis under anaerobiosis, concomitant with the stimulation of glycolysis, mediated in part by the activation of the $PP_i$-dependent phosphofructokinase by F-2,6-$P_2$ [5,30].

### 4.2. Structure-function analysis of COS $FBPase_c$

The purified COS $FBPase_c$ emitted low, but measurable, fluorescence when excited at 295 nm (results not shown). This is consistent with the existence of at least one tryptophan residue in the protein [22], as has been confirmed for the $FBPase_c$ from leaves of sugar beet, spinach and potato [18–20]. To determine whether the substrate or F-2,6-$P_2$ caused any structural alterations in the COS $FBPase_c$, the effect of these ligands on the enzyme's intrinsic fluorescence was examined.

The fluorescence studies indicated that F-1,6-$P_2$ titration causes two types of conformational changes in the COS $FBPase_c$. Low F-1,6-$P_2$ concentrations produced a small, but statistically reproducible, increase in fluorescence intensity, whereas substrate concentrations beyond 50 μM led to a progressive quenching of fluorescence emission (Fig. 2B). The former and latter appear to correspond to catalytic and inhibitory substrate binding, respectively (Fig. 2A). The presence of 0.5 μM F-2,6-$P_2$ negated fluorescence quenching attributed to inhibitory substrate binding while still allowing that ascribed to catalytic binding (Fig. 2D). Likewise, the presence of 1 mM F-1,6-$P_2$ negated fluorescence quenching due to F-2,6-$P_2$ (Fig. 4B). These data are indicative of the existence of a common substrate-inhibitory and F-2,6-$P_2$ binding site, and a distinct catalytic site in the COS $FBPase_c$. The fact that 1 mM F-1,6-$P_2$ and 2 μM F-2,6-$P_2$ produced similar hypochromic shifts without affecting the emission maximum (Fig. 1), agrees with the proposal that they produced similar structural changes in the enzyme mediated by their binding to a common inhibitory site.

Although X-ray crystallographic analyses of porcine kidney FBPase have suggested F-2,6-$P_2$ binding in the catalytic site [9,31], kinetic studies indicate that F-2,6-$P_2$ may bind at a distinct allosteric site [32]. Fig. 2A (and analogous data of other FBPases; i.e., see [32]) indicates that little substrate inhibition of COS $FBPase_c$ occurred in the presence of 0.5 μM F-2,6-$P_2$, and that the apparent $V_{max}$ obtained in the presence of 0.5 μM F-2,6-$P_2$ was equivalent to that of the maximally substrate-inhibited enzyme assayed in the absence of F-2,6-$P_2$. These kinetic data are consistent with the corresponding fluorescence results discussed above and presented in Fig. 2B–D, and lend support to the conclusion that inhibitory substrate and F-2,6-$P_2$ binding to COS $FBPase_c$ occurs at an identical site that is distinct from the enzyme's active site. This is in agreement with the reports that chemical modification of mammalian $FBPase_c$ using NEM eliminated substrate inhibitory and F-2,6-$P_2$ binding to an otherwise active enzyme [11–13]. The NEM-modified enzyme displayed a specific activity and $K_m$(F-1,6-$P_2$) that were similar to the F-2,6-$P_2$-inhibited native enzyme, consistent with NEM acting as an agonist in the F-2,6-$P_2$ inhibitory site.

Titration of COS $FBPase_c$ with F-2,6-$P_2$ resulted in progressive fluorescence quenching concomitant with kinetic inhibition of enzymatic activity (Fig. 4). The close agreement between respective $I_{50}$(F-2,6-$P_2$) and $K_d$(F-2,6-$P_2$) values (Table 1) indicates a direct correlation between inhibition and F-2,6-$P_2$ binding. Synergism between AMP and F-2,6-$P_2$ is demonstrated kinetically in Figs. 3 and 4A, and fluorometrically in Fig. 4B. Although we were unable to assess AMP binding to COS $FBPase_c$, a previous study with rabbit liver $FBPase_c$ indicated that AMP binding, measured using a fluorescent AMP analogue (formycin A-5′-P), was not altered by the presence of F-2,6-$P_2$ [7]. These findings indicate that although AMP enhances F-2,6-$P_2$ binding (Fig. 4B, Table 1), F-2,6-$P_2$ does not affect AMP binding by the enzyme [7]. The apparent sensitization of the enzyme to AMP inhibition by F-2,6-$P_2$ (Fig. 3, Table 1) must therefore arise from AMP assisting F-2,6-$P_2$ binding. This is reasonable since AMP binding promotes a pronounced R-to-T conformational transition [8] that could affect the distal (30 Å away) F-2,6-$P_2$ binding site. In contrast, binding of F-2,6-$P_2$, which elicits only minor conformational changes [9], is unlikely to have as pronounced an effect on the AMP allosteric site.

As AMP binding to FBPase causes a R-to-T conformational change leading to enhanced inhibition by F-2,6-$P_2$, and substrate inhibition appears to arise at the F-2,6-$P_2$ binding site, then AMP may also

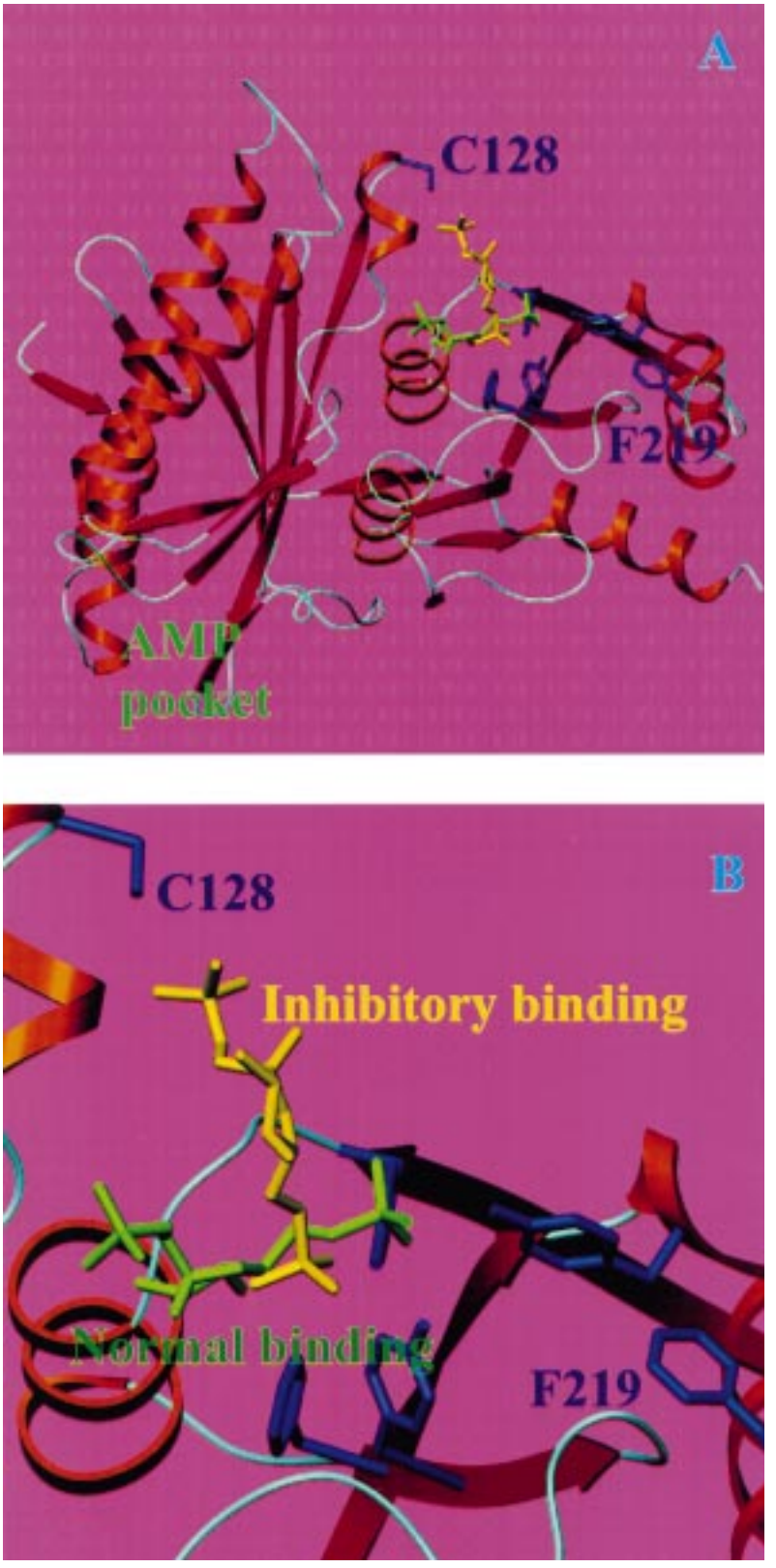
A
C128
F219
AMP
pocket
B
C128
Inhibitory binding
Normal binding
F219

enhance substrate inhibition. Indeed, the presence of 150 μM AMP reduced $FBPase_c$ activity at inhibitory F-1,6-$P_2$ concentrations in the range of 25–150 μM (Fig. 2A) indicating an increase in substrate inhibition. Similarly, the presence of 50 μM AMP promoted quenching of $FBPase_c$'s fluorescence attributed to inhibitory substrate binding (Fig. 2C). Thus, inhibition of $FBPase_c$ by AMP may be the result of increased substrate inhibition.

A model of FBPase inhibition that fits all of the available data requires the acknowledgement of a large body of X-ray crystal structure data from Lipscomb and his associates. Only one F-1,6-$P_2$ binding site has ever been observed [31] and F-2,6-$P_2$ appears to bind at the same site [9]. However, two F-1,6-$P_2$ binding sites have been indicated by our results (Fig. 2) and those of others [11–13]. Our modelling based on the pig kidney FBPase X-ray crystal structure (Fig. 5) also suggests that there may be an additional F-1,6-$P_2$ binding site. Cysteine-128, which is absolutely conserved in plant $FBPase_c$ [18–20], is about 12 Å away from the centre of the catalytic binding pocket (and represents the closest cysteine residue) (Fig. 5). A plausible site for inhibitory F-1,6-$P_2$ binding is created by moving the 1′-P end of the substrate close to cysteine-128 while keeping the 6′-P end more or less in the same location. Reasonable interactions can be achieved at this second binding site. From the X-ray studies [9,31] it is clear that the preferred binding site for low F-1,6-$P_2$ concentrations is the normal or catalytic binding site. However, F-2,6-$P_2$ or higher concentrations of F-1,6-$P_2$ could bind to a common inhibitory site. Since these two sites are mutually exclusive, under specific crystallization conditions which might favour one binding mode, the corresponding X-ray structure would only reveal one binding site (to our knowledge there has been no crystallographic experiment that involves a mixture of F-1,6-$P_2$ and F-2,6-$P_2$). Substrate inhibition may thus arise from F-1,6-$P_2$ binding at the F-2,6-$P_2$ inhibition site which overlaps with the catalytic site. Thus, inhibitory F-1,6-$P_2$ (or F-2,6-$P_2$) binding will sterically inhibit catalytic F-1,6-$P_2$ binding. The concept of overlapping binding sites has been previously suggested to account for the inhibition of mammalian FBPase by F-2,6-$P_2$ and F-1,6-$P_2$ [32].

The proposed F-1,6-$P_2$/F-2,6-$P_2$ inhibitory binding site illustrated in Fig. 5 is consistent with our fluorescence data obtained with the COS $FBPase_c$. There is a cluster of aromatic residues in the vicinity of the 6′-P end of F-1,6-$P_2$ (Fig. 5). All plant $FBPase_c$s that have been examined to date contain an absolutely conserved tryptophan residue in this region which corresponds to phenylalanine-219 of the mammalian FBPase [18–21]. As shown in Fig. 5, the interaction between the 6′-P and the aromatic cluster would slightly differ during catalytic F-1,6-$P_2$ binding versus inhibitory F-1,6-$P_2$ or F-2,6-$P_2$ binding. We suggest that the interaction that arises from the inhibitory binding mode has a quenching effect on the intrinsic fluorescence of the plant $FBPase_c$. NEM modification studies of mammalian FBPase [11–13] can also be readily explained by the model depicted in Fig. 5. A large group attached to cysteine-128 which is fully solvent exposed for efficient NEM modification would create steric hindrance for inhibitory F-1,6-$P_2$/F-2,6-$P_2$ binding without having much influence on catalytic F-1,6-$P_2$ binding.

The application of intrinsic fluorescence has provided quantitative structural evidence to complement the kinetic and regulatory characteristics of COS $FBPase_c$, as well as X-ray crystallographic and chemical modification analyses of mammalian FBPase. Potentially, intrinsic fluorescence studies of plant $FBPase_c$ could be used to help elucidate a more complex model of FBPase structure-function which includes the role of metals.

←

Fig. 5. A model depicting overlapping sites for catalytic and inhibitory F-1,6-$P_2$ binding to porcine kidney FBPase. (A) Overall view of the protein and its active and AMP binding sites. (B) Close-up view of the two binding sites. The model was generated using SETOR [33]. Coordinates of porcine kidney FBPase complexed with F-1,6-$P_2$ (PDB code 1FPB) were used. Normal (i.e., catalytic) F-1,6-$P_2$ binding is shown in green and reflects the crystallographic results. The proposed inhibitory binding is shown in yellow. Residues cysteine-128 and phenylalanine-219 are labelled.

## Acknowledgements

This work was supported by the Natural Sciences and Engineering Research Council of Canada (NSERC). We are also grateful to Prof. Vern L. Schramm (Dept. of Biochemistry, Albert Einstein College of Medicine) for the gift of formycin A-5′-P.

## References

[1] G.A. Tejwani, Adv. Enzymol. 54 (1983) 121–194.
[2] A.M. Vargas, M.M. Sola, M. Bounias, J. Biol. Chem. 265 (1990) 15368–15370.
[3] K. Skaleci, W. Mularczyk, A. Dzugaj, Biochem. J. 310 (1995) 1029–1035.
[4] R.J. Hodgson, W.C. Plaxton, FEBS Lett. 368 (1995) 559–562.
[5] W.C. Plaxton, Annu. Rev. Plant Physiol. Plant Mol. Biol. 47 (1996) 185–214.
[6] F. Lui, H.J. Fromm, J. Biol. Chem. 263 (1988) 9122–9128.
[7] J.E. Scheffler, H.J. Fromm, Biochemistry 25 (1986) 6659–6665.
[8] J.-Y. Liang, Y. Zhang, S. Huang, W.N. Lipscomb, Proc. Natl. Acad. Sci. USA 90 (1993) 2132–2136.
[9] J.-Y. Liang, S. Huang, Y. Zhang, H. Ke, W.N. Lipscomb, Proc. Natl. Acad. Sci. USA 89 (1992) 2404–2408.
[10] Y. Xue, S. Huang, J.-Y. Liang, Y. Zhang, W.N. Lipscomb, Proc. Natl. Acad. Sci. USA 91 (1994) 12482–12486.
[11] A. Reyes, M.E. Burgos, E. Hubert, J.C. Slebe, J. Biol. Chem. 262 (1987) 8451–8454.
[12] D.W. Meek, H.G. Nimmo, FEBS Lett. 160 (1983) 105–109.
[13] A. Reyes, E. Hubert, J.C. Slebe, Biochem. Biophys. Res. Commun. 127 (1985) 337–379.
[14] J. Daie, Photosynth. Res. 38 (1993) 5–14.
[15] G.B.G. Moorhead, R.J. Hodgson, W.C. Plaxton, Arch. Biochem. Biophys. 312 (1994) 326–335.
[16] M.J. Kobr, H. Beevers, Plant Physiol. 47 (1971) 48–52.
[17] D.T. Canvin, H. Beevers, J. Biol. Chem. 236 (1961) 988–995.
[18] C. Harn, J. Daie, Plant Physiol. 98 (1992) 790–791.
[19] Y. Hur, E.A. Unger, A.C. Vasconcelos, Plant Mol. Biol. 18 (1992) 799–802.
[20] R. Zrenner, K.P. Krause, P. Apel, U. Sonnewald, Plant J. 9 (1996) 671–681.
[21] F. Marcus, I. Edelstein, I. Reardon, R.L. Heinrikson, Proc. Natl. Acad. Sci. USA 79 (1982) 7161–7165.
[22] J.R. Lakowicz, Principles of Fluorescence Spectroscopy, Plenum Press, New York, 1983.
[23] J.Y. Su, K.B. Storey, Biochem. Cell Biol. 71 (1993) 255–259.
[24] J.V. Passoneau, O.H. Lowry, Enzymatic Analysis: a Practical Guide, Humana Press, Totowa, NJ, 1993.
[25] S.P.J. Brooks, Biotechniques 13 (1992) 906–911.
[26] R.M.C. Dawson, D.C. Elliott, W.H. Elliot, K.M. Jones, Data For Biochemical Research, 3rd edn., Clarendon Press, Oxford, 1986.
[27] N.J. Kruger, H. Beevers, Plant Physiol. 76 (1984) 49–54.
[28] E. Van Shaftingen, H.G. Hers, Proc. Natl. Acad. Sci. USA 78 (1981) 2861–2863.
[29] N.J. Kruger, H. Beevers, Plant Physiol. 77 (1985) 358–364.
[30] E. Kombrink, N.J. Kruger, H. Beevers, Plant Physiol. 74 (1984) 395–401.
[31] U. Zhang, J.-Y. Liang, S. Huang, H. Ke, W.N. Lipscomb, Biochemistry 32 (1993) 1844–1857.
[32] E. Van Schaftingen, Adv. Enzymol. 59 (1987) 315–395.
[33] S.V. Evans, J. Mol. Graph. 11 (1993) 134–138.